Oxidative Remodeling of Chromoplast Carotenoids: Identification of the Carotenoid Dioxygenase *CsCCD* and *CsZCD* Genes Involved in Crocus Secondary Metabolite Biogenesis

Florence Bouvier,[a] Claude Suire,[b] Jérôme Mutterer,[a] and Bilal Camara[a,1]

[a] Institut de Biologie Moléculaire des Plantes, Centre National de la Recherche Scientifique and Université Louis Pasteur, 67084 Strasbourg Cedex, France
[b] Institut de Biochimie et Génétique Cellulaires, Centre National de la Recherche Scientifique, 33077 Bordeaux Cedex, France

The accumulation of three major carotenoid derivatives—crocetin glycosides, picrocrocin, and safranal—is in large part responsible for the color, bitter taste, and aroma of saffron, which is obtained from the dried styles of Crocus. We have identified and functionally characterized the Crocus zeaxanthin 7,8(7′,8′)-cleavage dioxygenase gene (*CsZCD*), which codes for a chromoplast enzyme that initiates the biogenesis of these derivatives. The Crocus carotenoid 9,10(9′,10′)-cleavage dioxygenase gene (*CsCCD*) also has been cloned, and the comparison of substrate specificities between these two enzymes has shown that the CsCCD enzyme acts on a broader range of precursors. *CsZCD* expression is restricted to the style branch tissues and is enhanced under dehydration stress, whereas *CsCCD* is expressed constitutively in flower and leaf tissues irrespective of dehydration stress. Electron microscopy revealed that the accumulation of saffron metabolites is accompanied by the differentiation of amyloplasts and chromoplasts and by interactions between chromoplasts and the vacuole. Our data suggest that a stepwise sequence exists that involves the oxidative cleavage of zeaxanthin in chromoplasts followed by the sequestration of modified water-soluble derivatives into the central vacuole.

INTRODUCTION

Carotenoids are isoprenoid pigments that have key biological functions in organisms of all major taxa. The oxidation of the rigid backbone of carotenoids by specific dioxygenases leads to the formation of diverse bioactive derivatives such as vitamin A (von Lintig and Vogt, 2000; Wyss et al., 2000), the plant hormone abscisic acid (Schwartz et al., 1997), and several aroma compounds (Enzell, 1985; Buttery et al., 1988; Sefton et al., 1989; Winterhalter and Rouseff, 2002) and apocarotenoid pigments (Winterhalter and Rouseff, 2002). In plants, this metabolic process generally is stimulated during flowering (Eugster and Märki-Fischer, 1991), fruit ripening (Gross and Eckhardt, 1981; Lutz and Winterhalter, 1992; Maoka et al., 2001; Fleischmann et al., 2002), industrial curing of tobacco (Wahlberg et al., 1977), and tea fermentation (Kawakami and Kobayashi, 2002).

Crocus, a cultivated sterile plant, offers a convenient model with which to further our understanding of this carotenoid catabolic pathway. Upon flowering in autumn, Crocus displays red style branches (Figures 1A and 1B), which once dry constitute the spice saffron (Mathew, 1983). Saffron is the most expensive spice known and also is a valuable herbal medicine (Gainer and Brumgard, 1982; Sampathu et al., 1984; Holloway and Gainer, 1988). The accumulation of three major carotenoid derivatives—crocetin glycosides, picrocrocin, and safranal—is in large part responsible for the unique color, bitter taste, and aroma of saffron (Figure 1C) (Winterhalter and Rouseff, 2002). Stereochemical configurations (Buchecker and Eugster, 1973) and a highly reduced carotenoid level in saffron suggest that these secondary metabolites are formed by an unusual sequence that involves the cleavage of zeaxanthin (Pfander and Schurtenberger, 1982) followed by oxidative modifications and glycosylations (Figure 1C). Although these compounds generate much interest, enzymes that initiate the reaction sequence have not been identified.

The limited occurrence of crocetin and related apocarotenoids in nature (Eugster et al., 1969; Tandon et al., 1979; Pfister et al., 1996; Liao et al., 1999) argues against their
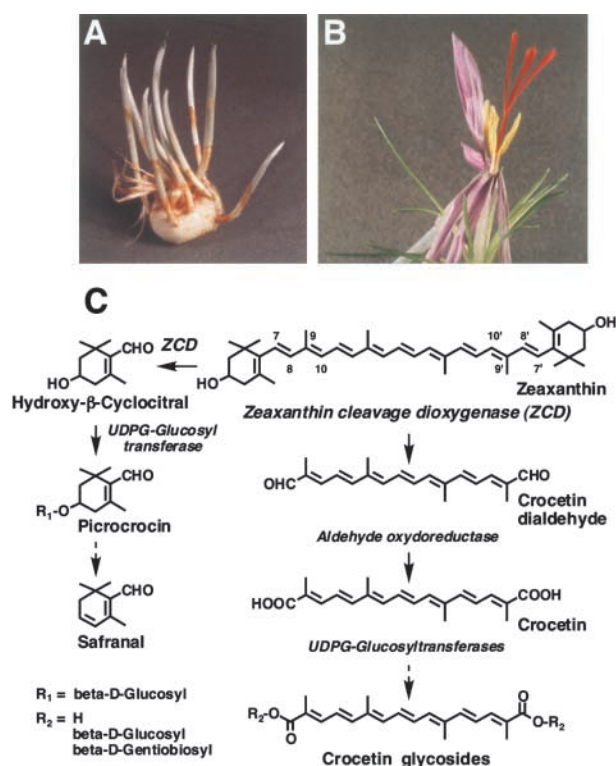
Figure 1. Accumulation and Pathway of Carotenoid-Derived Metabolites in Crocus.

(A) Perianth tubes sprouting from the corm.
(B) Crocus flower displaying red style branches that accumulate carotenoid-derived metabolites.
(C) Possible pathway for the biosynthesis of carotenoid metabolites in Crocus style branches. Zeaxanthin, the postulated precursor, is cleaved and modified by different enzymes, which are listed in italics.

synthesis via an enzymatic cooxidation mechanism involving ubiquitous lipoxygenases (Wu et al., 1999) or xanthine oxidases (Bosser and Belin, 1994). Two types of carotenoid cleavage dioxygenases have been identified in plants. The first is the maize Vp14 (Schwartz et al., 1997), which catalyzes the conversion of epoxy-xanthophylls to the abscisic acid precursor xanthoxin. The second is the Arabidopsis broad-substrate-specificity carotenoid dioxygenase (AtCCD1), which cleaves the 9,10 and 9′,10′ double carbon-carbon bonds of carotenoid chromophores (Schwartz et al., 2001). However, none of these enzymes cleaves the carotenoid chromophore at the 7,8 and 7′,8′ positions (Figure 1C). These two positions have the highest electron density in the carotenoid chromophore (El-Tinay and Chichester, 1970) and represent potential targets of Crocus dioxygenase, which leads to the formation of secondary saffron metabolites.

Here, we report the discovery and the functional characterization of two Crocus carotenoid cleavage dioxygenases, CsCCD (carotenoid cleavage dioxygenase) and CsZCD (zeaxanthin cleavage dioxygenase). We demonstrate that CsCCD is a member of the broad-substrate-specificity 9,10(9′,10′)-carotenoid cleavage dioxygenase involved in the synthesis of several carotenoid-derived metabolites (Schwartz et al., 2001; Winterhalter and Rouseff, 2002), whereas, CsZCD specifically catalyzes the synthesis of crocetin dialdehyde and hydroxy-β-cyclocitral from zeaxanthin. Thus, CsZCD is the Crocus 7,8(7′,8′)-zeaxanthin cleavage dioxygenase that initiates the synthesis of saffron pigment and aroma (Figure 1C). Further immunological and gene expression analyses revealed that unlike CsCCD, CsZCD is expressed specifically in the chromoplasts of style cells during the active period of zeaxanthin cleavage. We also investigated the ultrastructural changes in the style during the synthesis of secondary saffron metabolites. Our results have led to the hypothesis that in Crocus styles, the carotenoid-derived metabolites are sequestered in the vacuole, consistent with their water-soluble nature.

RESULTS

Carotenoid Analysis of Crocus Style Branches

We analyzed the carotenoid content in red Crocus style branches to evaluate the oxidative pathway that leads to the synthesis of carotenoid-derived metabolites in saffron (Pfander and Schurtenberger, 1982) (Figure 1C). This analysis was performed by subjecting the ethanol extract prepared from the style branches to HPLC separation and then evaluating the structural identities of the separated metabolites based on their diode-array spectra. This revealed the presence of picrocrocin (Figures 2A and 2B) and three major crocetin glycosides (Figures 2C and 2D). The HPLC gradient (II) was used to profile the full spectrum of C_{40} carotenoids, but the presence of β-carotene and zeaxanthin, which were isolated previously from Crocus (Pfander and Schurtenberger, 1982), was not detected. Therefore, the C_{20} apocarotenoid crocetin, which might be derived from zeaxanthin, is responsible for the brilliant red color of the style branches of Crocus.

Cloning of the Cleavage Dioxygenase Genes *CsCCD* and *CsZCD*

Based on the peptide sequence of Vp14 and the related peptide sequence of pepper and *Synechocystis* sp PC6803, we prepared forward and reverse oligonucleotides, which are complementary to the conserved AHPKVDP and HD-

FAITE regions, to reverse transcribe and amplify the cDNA fragments from the mRNA of Crocus style branches. After sequence analysis, two specific 171- and 177-bp DNA probes were isolated and used to screen a cDNA library from Crocus style branches, as described in Methods. This led to the isolation of two clones (1200 and 750 bp) devoid of the 5′ and 3′ regions. The missing regions were obtained by rapidly amplifying the cDNA ends. Two full-length cDNAs were identified and tentatively named *CsCCD* and *CsZCD*.

The cDNA sequence of *CsCCD* is 1686 bp long with an open reading frame coding for a protein of 546 amino acids and has an estimated molecular mass of 62 kD, whereas *CsZCD* is 1186 bp long, codes for a protein of 369 amino acids, and has a molecular mass of 41 kD (Figure 3). Sequence comparison revealed that 27% of the deduced amino acid sequence of *CsCCD* is identical to that of CsZCD (Figure 3). CsCCD is 77% identical to a partial EST

from Crocus. The same level of sequence identity is observed with the pepper CaCCD and Arabidopsis carotenoid dioxygenase AtCCD1 (Schwartz et al., 2001). CsZCD shows strong identity (97%) to a partial Crocus EST and low but significant identity (44%) to an apple flower protein of unknown function (Watillon et al., 1998).

The deduced peptide sequences of CsCCD and CsZCD cDNAs did not reveal characteristic plastid transit peptide patterns (Gavel and von Heijne, 1990). To determine where CsCCD and CsZCD localize in situ, we analyzed the tissue sections of Crocus style branches by immunocytochemical staining and confocal microscopy using antibodies developed against synthetic peptide sequences specific for CsCCD and CsZCD. Confocal microscopy using anti-CsCCD antibodies revealed a staining pattern consistent with a cytosolic location (Figure 4A). In the case of the control sample treated with the preimmune serum, no specific
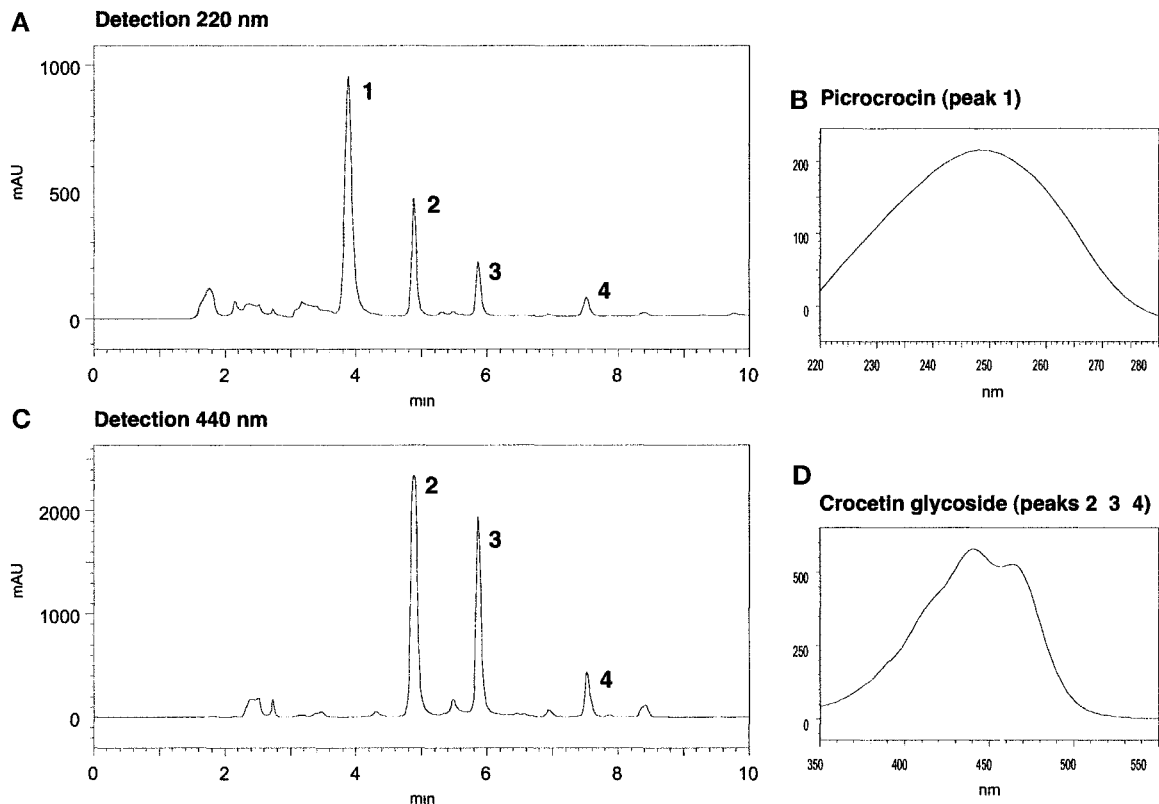

Figure 2. HPLC Analysis of Carotenoid-Derived Metabolites from Crocus Style Branches.

(A) HPLC analysis of Crocus style extracts. Compounds were detected by UV-light absorbance at 220 nm. Peak 1 corresponds to picrocrocin, and peaks 2 to 4 correspond to crocetin carrying different glycosyl residues.
(B) Online diode-array spectrum of picrocrocin. For peaks 2 to 4, see **(D)**.
(C) HPLC analysis of carotenoid-derived metabolites from Crocus style. Compounds were detected by visible light absorbance at 440 nm. Peaks 2 to 4 correspond to crocetin carrying different glycosyl residues.
(D) Typical online diode-array spectrum of crocetin glycoside (peak 2). The profiles of peaks 3 and 4 were similar.
Chromatographic separation was performed using gradient I (see Methods). mAU, milliabsorbance units.
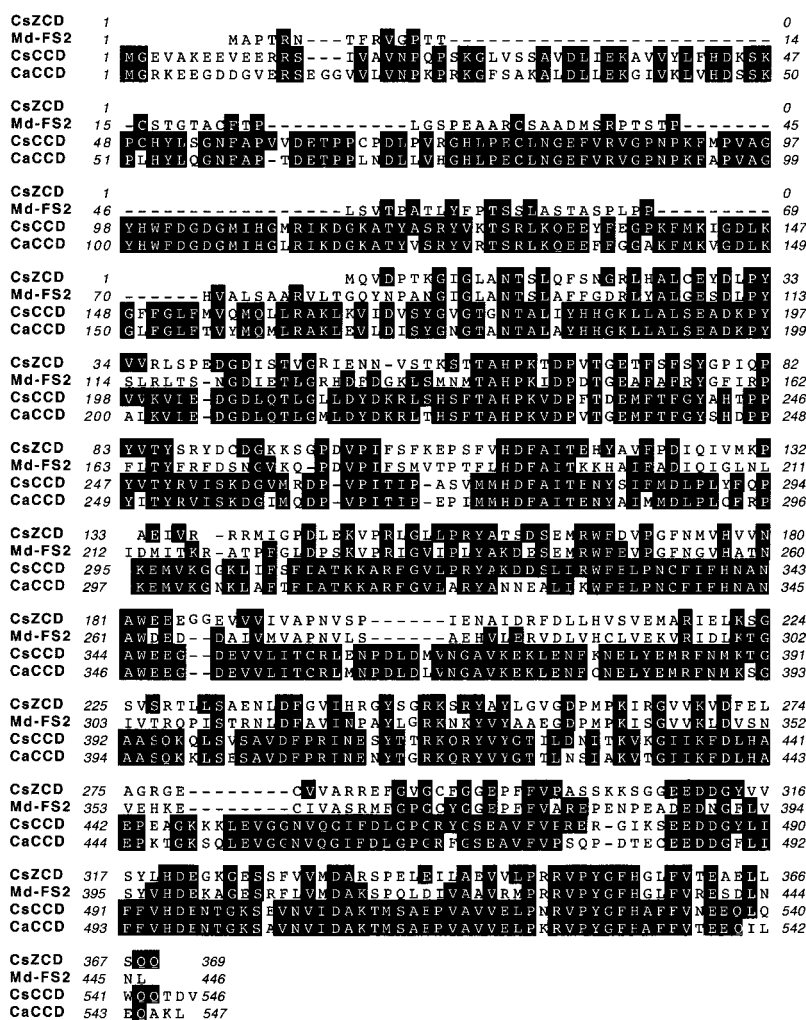
```
CsZCD    1                       MAPTRN---TFRVGPTT                      0
Md-FS2   1                       MAPTRN---TFRVGPTT                      14
CsCCD    1    MGEVAKEEVEERRS---IVAVNPQPSKGLVSSAVDLIEKAVVYLHDKSK    47
CaCCD    1    MGRKEEGDDGVERSEGGVVLVNPKPRKGFSAKAIDLLEKGIVKLVHDSSK   50

CsZCD    1                                                                0
Md-FS2   15   -CSTGTACFTP-------------LGSPEAARCSAADMSRPTSTP-------  45
CsCCD    48   PCHYLSGNFAPVVDETPPCPDIPVRGHLPECLNGEFVRVGPNPKFMPVAG   97
CaCCD    51   PLHYLQGNFAP-TDETPPLNDLLVHGHLPECLNGEFVRVGPNPKFAPVAG   99

CsZCD    1                                                                0
Md-FS2   46   -------------------LSVTPATLYFPTSSIASTASPLPP--------- 69
CsCCD    98   YHWFDGDGMIHGMRIKDGKATYASRYVKTSRLKOEEYFEGPKFMKIGDLK   147
CaCCD    100  YHWFDGDGMIHGLRIKDGKATYVSRYVRTSRLKQEEFFGGAKFMKVGDLK   149

CsZCD    1                      MQVDPTKGIGLANTSLQFSNGRLHALCEYDLPY     33
Md-FS2   70   ------HVALSAARVLTGQYNPANGIGLANTSLAFFGDRLYALCESDIPY   113
CsCCD    148  GFFGLFMVQMQLLRAKLKVIDVSYGVGTGNTALIYHHGKLLALSEADKPY   197
CaCCD    150  GLFGLFTVYMQMLRAKLPVIDISYGNGTANTALAYHHGKLLALSEADKPY   199

CsZCD    34   VVRLSPEDGDISTVGRIENN-VSTKSTTAHPKTDPVTGETTSFSYGPIQP   82
Md-FS2   114  SLRLTS-NGDIETLGREDFDGKLSMNMTAHPKIDPDTGEAFAFRYGFIRP   162
CsCCD    198  VVKVIE-DGDLQTLGLLDYDKRLSHSFTAHPKVDPFTDEMFTFGYAHTPP   246
CaCCD    200  AIKVIE-DGDLQTLGMLDYDKRLTHSFTAHPKVDPVTGEMFTFGYSHDPP   248

CsZCD    83   YVTYSRYDCDGKKSGDDVPIFSFKEPSFVHDFAITEHYAVFPDIQIVMKP   132
Md-FS2   163  FLTYFRFDSNCVKQ-PDVPIFSMVTPTFLHDFAITKKHAIFADIQIGLNL   211
CsCCD    247  YVTYRVISKDGVMRDP-VPITIP-ASVMMHDFAITENYSIFMDLYFQP     294
CaCCD    249  YITYRVISKDGIMQDP-VPITIP-EPIMMHDFAITENYAIMMDLPLQFRRP  296

CsZCD    133  AEIVR-RRMIGPDLEKVPRLGLLPRYATSDSEMRWFDVPGFNMVHVVN    180
Md-FS2   212  IDMITKR-ATPFGLDPSKVPRIGVIPIYAKDPSEMRWFEVPGFNGVHATN   260
CsCCD    295  KEMVKGCKLIFSFIATKKARFGVLPRYAKDDSLIRWFELPNCFIFHNAN    343
CaCCD    297  KEMVKGNKLAFTFIATKKARFGVLARYANNEALIKWFELPNCFIFHNAN    345

CsZCD    181  AWEEEGGEVVVIVAPNVSP------IENAIDRFDLLHVSVEMARIELKSG   224
Md-FS2   261  AWDED--DAIVMVAPNVLS------AEHVLPRVDLVHCLVEKVRIDLKTG   302
CsCCD    344  AWEEG--DEVVLITCRLPNPDLDMVNGAVKEKLENFKNELYEMRFNMKTG   391
CaCCD    346  AWEEG--DEVVLITCRLPNPDLDLVNGAVKEKLENFCNELYEMRFNMKSG   393

CsZCD    225  SVSRTLLSAENLDFGVLHRGYSGRKSRYAYLGVGDPMPKIRGVVKVDFEL   274
Md-FS2   303  IVTRQPISTRNLDFAVINPAYLGRKNKYVVAAEGDPMPKISGVVKIDVSN   352
CsCCD    392  AASQKQLSVSAVDFPRINESYTTRKORYVYGTILDNITKVKGIIKFDLHA   441
CaCCD    394  AASQKKLSESAVDFPRINENYTGRKQRYVYGTTLNSIAKVTGIIKFDLHA   443

CsZCD    275  AGRGE--------CVVARREFGVGCFGGEPFFVPASSKKSGEEDDGYVV    316
Md-FS2   353  VEHKE--------CIVASRMFGPGCYGGEPBFVAREPENPEADEDRGFLV   394
CsCCD    442  EPEAGKKKLEVGGNVQGIFDLCPCRYCSEAVFVFRER-GIKSEEDDGYLI   490
CaCCD    444  EPKTGKSQLEVGCNVQGIFDLQPCRFGSEAVFVPSQP-DTECEEDDGFLI   492

CsZCD    317  SYLHDEGKGESSFVVMDARSPELEIILAEVVLPRRVPYGFHGLFVTEAELL  366
Md-FS2   395  SYVHDEKAGESRFIVMDAKSPQLDIVAAVRMPRRVPYGFHGLFVRESDLN   444
CsCCD    491  FFVHDENTGKSEVNVIDAKTMSAEPVAVVELPNRVPYGFHAFFVNEEQLQ   540
CaCCD    493  FFVHDENTGKSAVNVIDAKTMSAEPVAVVELPKRVPYGFHAFFVTEEQIL   542

CsZCD    367  SQQ        369
Md-FS2   445  NL         446
CsCCD    541  WQQTDV     546
CaCCD    543  EQAKL      547
```

Figure 3. Comparison of the Predicted Amino Acid Sequences of Crocus Carotenoid Cleavage Dioxygenases and Related Proteins.

CsZCD and CsCCD are carotenoid cleavage dioxygenases from Crocus. Md-FS2 is an apple flower protein of unknown function (Watillon et al., 1998). CaCCD is a pepper homolog of Arabidopsis cleavage dioxygenase (Schwartz et al., 2001). Identical amino acids are indicated with black backgrounds.

staining pattern was detected (Figure 4B). On the other hand, antibodies directed against CsZCD revealed a specific labeling of plastids (Figure 4C), which was not observed when the tissue sections were treated with the preimmune serum (Figure 4D).

Identification of *CsCCD* as a Carotenoid 9,10(9′,10′)-Cleavage Dioxygenase

To determine whether *CsCCD* cDNA codes for a carotenoid cleavage dioxygenase, CsCCD was expressed heterologously in *Escherichia coli* as a fusion protein with a molecular mass of 75 kD on SDS gels (Figure 5A). Purified recombi-

nant protein from bacterial cultures induced at 20°C (Figure 5A) was assayed for its cleavage activity using zeaxanthin as a substrate. After incubation and thin layer chromatography analysis, a new product ($R_F = 0.65$) was detected that showed intense orange fluorescence under UV light. The product also showed purple to red fluorescence when the plate was sprayed with dinitrophenylhydrazine reagent, revealing the presence of a carbonyl group (data not shown). No conversion was observed in the incubation medium containing the soluble protein isolated from *E. coli* transformed with the empty vector. The incubation mixture was analyzed further by reverse-phase HPLC along with diode-array detection (Figures 5B to 5E). This analysis showed that the product was adsorbed poorly on the hydrophobic reverse

phase (Figure 5B, peak 2) and displayed a chromophore structure (Figure 5C).

The UV-visible light spectrum in hexane, with the maximum wavelength (λmax) at 356, 374, and 396 nm (Figure 5F), is characteristic of a pentaene chromophore (Vetter et al., 1971). The fine structure of the spectrum disappeared in ethanol (Figure 5G) and was restored after the reduction of carbonyl groups with sodium borohydride (Figure 5H). This finding indicated the presence of carbonyl groups conjugated with a chromophore structure (Critchley et al., 1958). The absorbance maxima of the reduced product (λmax at 324, 340, and 359 nm) (Figure 5H) were identical to those reported for rosafluine (Märki-Fischer and Eugster, 1988). The structure was further confirmed by mass spectrometry, which revealed a prominent molecular ion of 216 mass units corresponding to $C_{14}H_{16}O_2$ (Figure 6) and a fragmentation pattern consistent with the structure (Enzell et al., 1969). These characteristics indicate that the new zeaxanthin derivative is similar to the C_{14} dialdehyde 4,9-dimethyldodeca-2,4,6,8,10-pentaene-1,12-dialdehyde (Isler et al., 1956). Collectively, these results demonstrate that *CsCCD* is a carotenoid 9,10(9′,10′)-cleavage dioxygenase that catalyzes the formation of 4,9-dimethyldodeca-2,4,6,8,10-pentaene-1,12-dialdehyde and probably hydroxydihydro-β-ionone from zeaxanthin.

Identification of CsZCD as the Zeaxanthin 7,8(7′,8′)-Cleavage Dioxygenase

We cloned the *CsZCD* cDNA in frame with a polyhistidine affinity tag of the pBAD/TOPO ThioFusion vector and expressed the recombinant protein in *E. coli* cultured at 20°C,

Figure 4. Immunohistochemical Localization of Carotenoid Cleavage Dioxygenases in Crocus Style Branches.

(A) and **(B)** Style sections incubated with anti-CsCCD antibody **(A)** and preimmune CsCCD serum **(B)**. Bars = 50 μm.
(C) and **(D)** Style sections incubated with anti-CsZCD antibody **(C)** and preimmune CsZCD serum **(D)**. Bars = 5 μm.
The images were obtained using confocal laser-scanning microscopy.

as described above for CsCCD. The affinity-purified fusion protein migrated on SDS gels as a polypeptide with a molecular mass of 55 kD (Figure 7A). When the purified protein was incubated with various carotenoid substrates, we observed that zeaxanthin was cleaved to yield a new nonfluorescent product (R_F = 0.73) that gave a positive reaction when the plate was sprayed with dinitrophenylhydrazine (Figure 7B). Under our incubation conditions, *cis*- and *trans*-violaxanthin apparently were not transformed into colored products (Figure 7B). Soluble proteins from *E. coli* cells carrying the empty vector failed to transform zeaxanthin (Figure 7B). Like the C_{14} dialdehyde mentioned above, the CsZCD product behaved anomalously by reverse-phase HPLC (Figures 7C to 7E). The UV-visible light spectrum revealed λmax at 405, 430, and 458 nm in hexane (Figure 7F). The fine structure of the UV-visible light spectrum disappeared in ethanol (Figure 7G) and was restored after borohydride reduction, as shown by the λmax at 375, 395, and 421 nm (Figure 7H). These characteristics are consistent with an 8,8′-diapocarotene 8,8′-diapocarotenone structure (Vetter et al., 1971). This structure was confirmed by mass spectrometry analysis, which showed a molecular ion of 296 mass units and characteristic fragments (Figure 8). Such a molecular mass and fragmentation pattern are consistent with the structure of crocetin dialdehyde ($C_{20}H_{24}O_2$) (Enzell et al., 1969; Vetter et al., 1971; Jüttner and Höflatcher, 1985).

The functional activity of CsZCD was confirmed using a plasmid-based complementation procedure. We transformed *E. coli* (strain JM109) producing zeaxanthin with the *CsZCD* cDNA. After induction and overnight culture, the bacteria expressing the *CsZCD* cDNA developed a red color, which was not observed in the control strain (Figure 9A). HPLC analysis of the total lipid extract showed that zeaxanthin remained untransformed in the control strain (Figures 9B and 9C), whereas in bacteria expressing the *CsZCD* cDNA, zeaxanthin was converted to crocetin dialdehyde (Figures 9D and 9E). Further UV-visible light spectrophotometry and mass spectrometry analyses revealed that the crocetin dialdehyde produced in vivo was identical to that obtained in vitro (data not shown).

Developmental and Stress Regulation of CsCCD and CsZCD

Protein gel blot analysis was performed to analyze the tissue-specific expression patterns of *CsCCD* and *CsZCD* using polyclonal antibodies prepared against purified peptide sequences specific to each enzyme (see Methods). When the protein gel blot was probed with anti-CsCCD, a single 60-kD band was detected in the vegetative and floral tissues of Crocus (Figure 10A). On the other hand, anti-CsZCD revealed a single 40-kD protein in the style branches only (Figure 10A), in accordance with its physiological role in this tissue.

The expression of *CsCCD* and *CsZCD* was studied by RNA gel blot analysis using various Crocus tissues. Figure
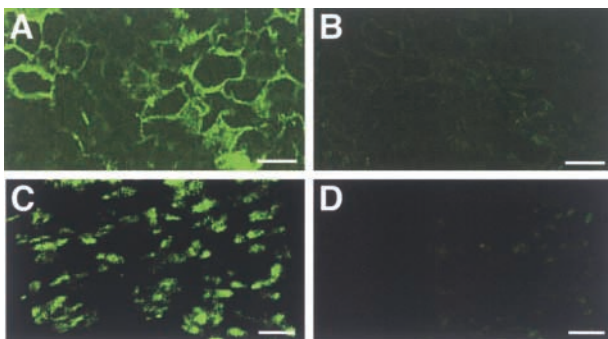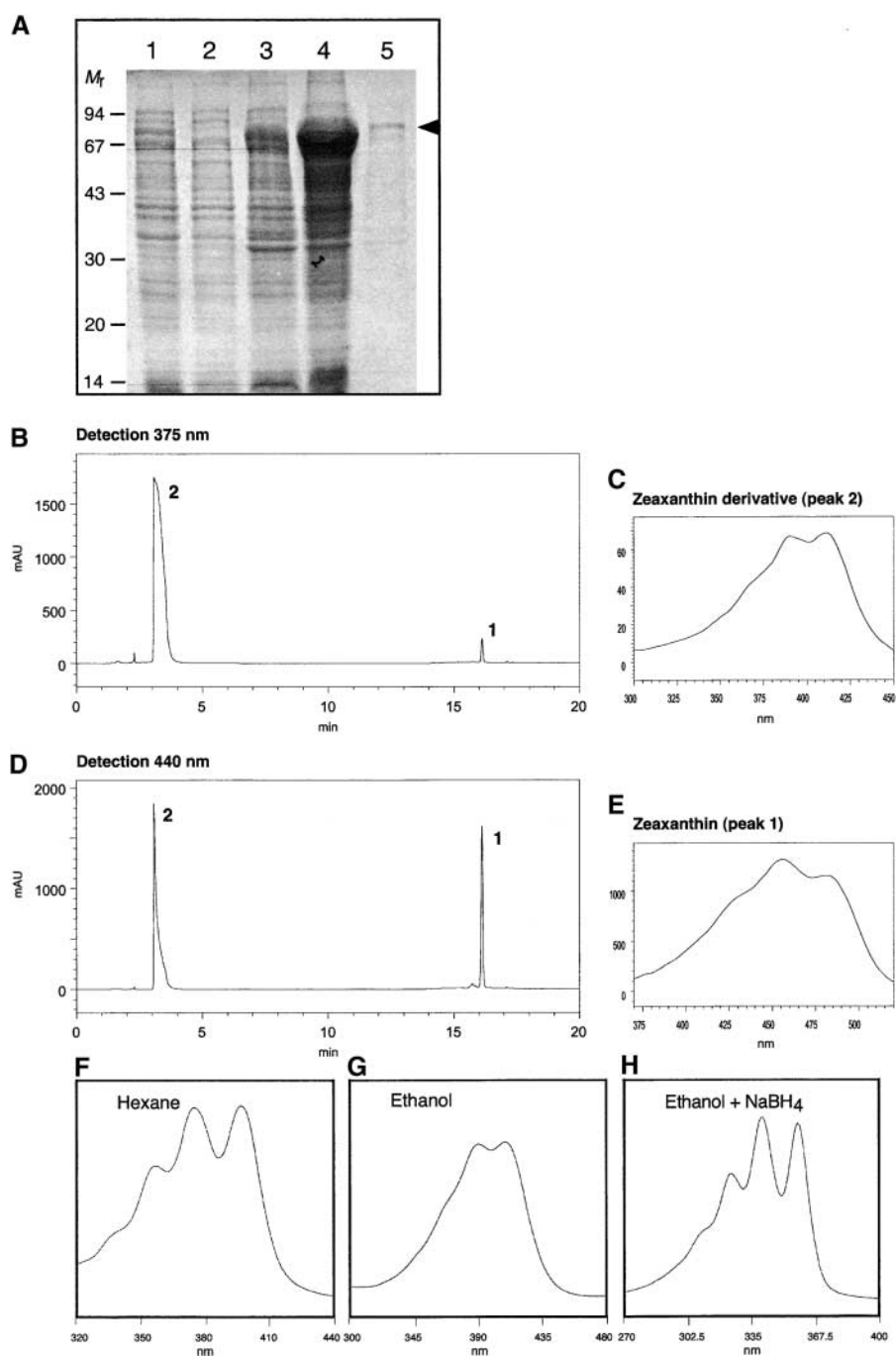
Figure 5. Functional Analysis of Recombinant CsCCD Reaction Products.

(A) SDS-PAGE analysis of affinity-purified CsCCD. Soluble protein from bacteria grown at 20°C (lane 1) and 37°C (lane 2) and insoluble protein from bacteria grown at 20°C (lane 3) and 37°C (lane 4) were examined. Affinity-purified fusion protein was loaded in lane 5 (arrowhead). MW, molecular mass.

(B) to **(E)** HPLC results (monitored at 375 nm **[B]** and 440 nm **[D]**) and online diode-array spectra of CsCCD reaction products. The separation of zeaxanthin (peak 1) and its cleavage derivative (peak 2) and online diode-array spectra of peak 2 **(C)** and zeaxanthin **(E)** are shown. mAU, milliabsorbance units.

(F) to **(H)** UV-visible light spectra of the reaction product (peak 2) in hexane **(F)** and in ethanol before **(G)** and after **(H)** reduction with sodium borohydride.
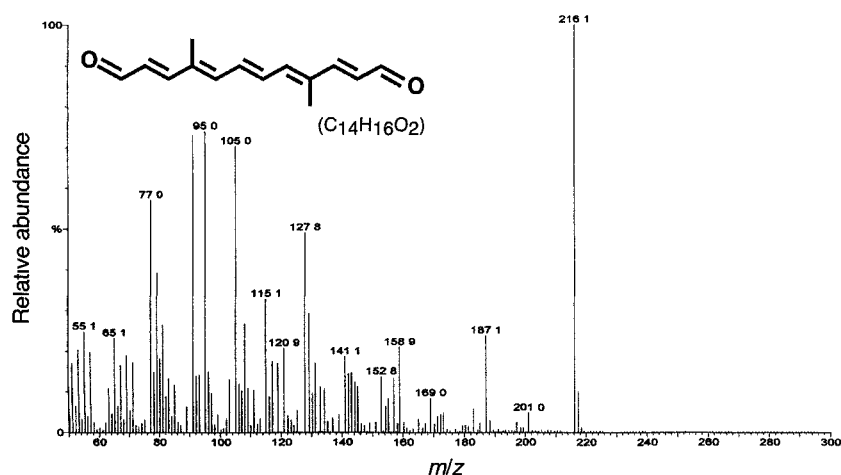
Figure 6. Full-Scan Mass Spectrometry of the Reaction Product of CsCCD.

Electron-impact mass spectrum of the reaction product (peak 2) obtained as shown in Figure 5B. m/z, mass-to-charge ratio.

10B shows that *CsCCD* was expressed constitutively at a low level in all tissues, whereas *CsZCD* was expressed specifically in the style branches. We also hybridized the same blot to Crocus cDNA that codes for the enzyme 1-deoxy-D-xylulose 5-phosphate reductoisomerase, which catalyzes the first specific steps of isopentenyl diphosphate synthesis in plastids. The 1-deoxy-D-xylulose 5-phosphate reductoisomerase gene was expressed largely in the style branches but to a lesser extent in petals and leaves (Figure 10B). To gain insight into the potential regulation of *CsZCD*, we dehydrated the style branches and analyzed the pattern of *CsZCD* transcript accumulation. The data shown in Figure 10C indicate that *CsZCD* was regulated positively by dehydration. To confirm that stress by dehydration influences *CsZCD* expression, we analyzed the transcript levels of genes reported previously to be involved in drought stress. These included the alternative oxidase (Maxwell et al., 1999), ascorbate peroxidase (Mittler and Zilinskas, 1994), calcineurin B (Kudla et al., 1999), and betaine aldehyde dehydrogenase (Ishitani et al., 1995). PCR primers corresponding to Crocus cDNA sequences (see Methods) were used to amplify the expected amplicon from reverse-transcribed RNAs of dehydrated style branches. These experiments were performed three times, and their results are shown in Figure 10C. The expression of *CsZCD* and the four stress-regulated genes was enhanced concomitantly in dehydrated style branches.

Plastid Differentiation during Carotenoid-Derived Metabolite Biogenesis

Because the massive synthesis of carotenoids generally is accompanied by plastid differentiation, we analyzed by electron microscopy the ultrastructure of Crocus style branch cells in relation to the intense accumulation of zeaxanthin-derived metabolites. Histochemical analysis revealed plastids that stain positively for polysaccharides (Thiéry, 1967) at the very beginning of Crocus style development. These polysaccharides appear as dark deposits because of their starch content (Figure 11A). At the ultrastructural level, numerous amylogenic proplastids were observed during this developmental period (Figure 11B). Subsequently, these proplastids differentiated into tubular chromoplasts (Figure 11C) and the starch was hydrolyzed, probably for the synthesis of zeaxanthin, which was cleaved by CsZCD. In the later stages of development, interactions and apparent transfer of secretory inclusions from chromoplasts to the vacuole were observed (Figures 11D to 11F). Thus, at the final stage of development, the water-soluble zeaxanthin derivatives apparently accumulated in the vacuole (Figure 11G).

DISCUSSION

Carotenoid Remodeling by Specific Dioxygenases

We have identified CsCCD and CsZCD, two functionally related enzymes involved in the production of Crocus secondary metabolites from zeaxanthin. *CsCCD* specifically cleaves the 9-10 and 9′-10′ double bond of carotenoid chromophores. Thus, this enzyme is homologous with Arabidopsis AtCCD1 (Schwartz et al., 2001). The substrate specificity of *CsCCD* may explain the presence of roseoside [(4-hydroxy-4-(3′-hydroxy-1′-butenyl)-3,5,5-trimethyl-2-cyclohexen-1-one 3′-O-β-glucopyranoside] (Straubinger et al., 1998) and 4-hydroxy-α-ionol (Winterhalter and Straubinger, 2000) in the aroma
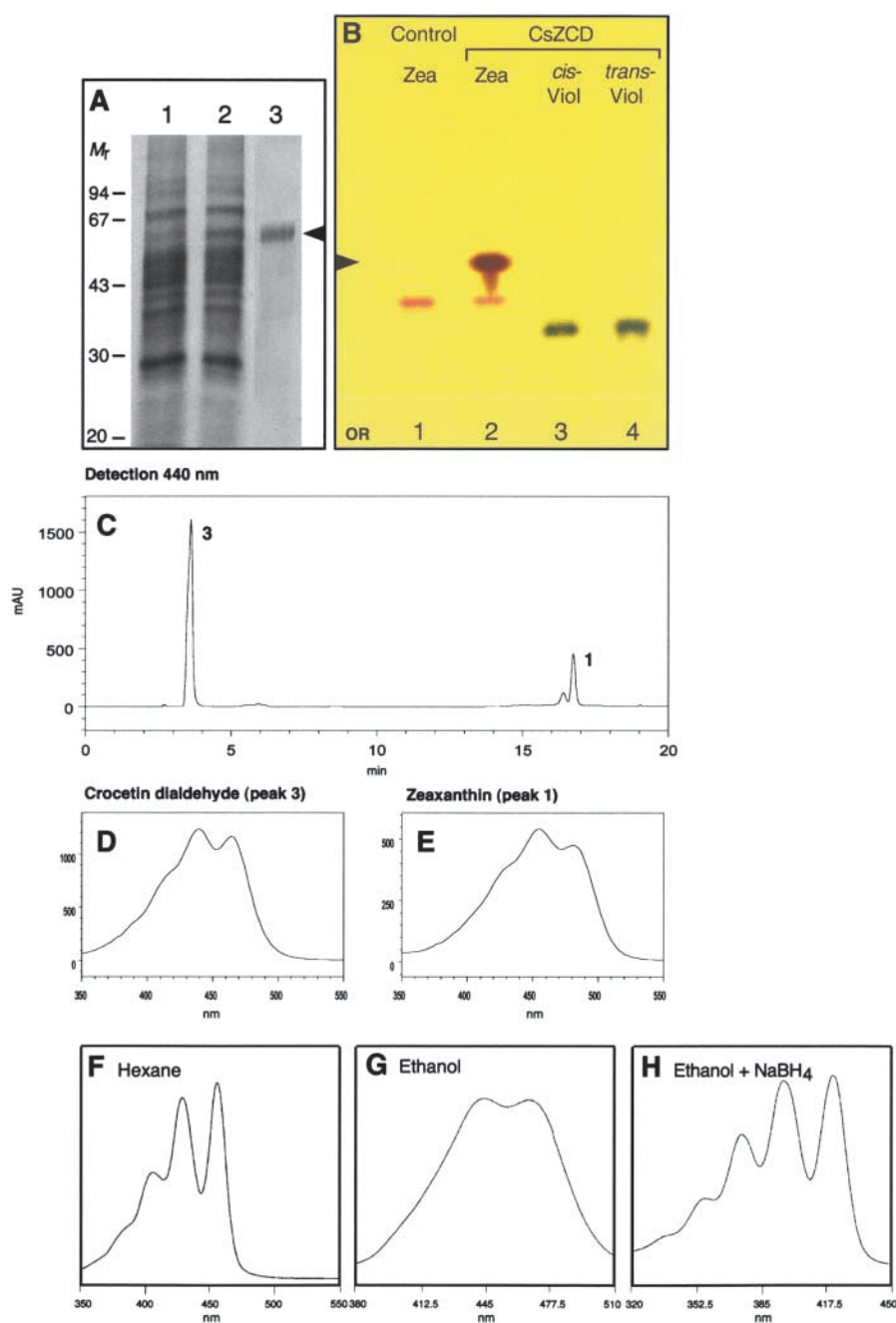
Figure 7. Functional Analysis of Recombinant CsZCD.

(A) SDS-PAGE analysis of affinity-purified CsZCD. Soluble protein from bacteria grown at 20°C without (lane 1) or after (lane 2) induction was examined. Lane 3 was loaded with affinity-purified CsZCD fusion protein (arrowhead). MW, molecular mass.

(B) Thin layer chromatography analysis of CsZCD reaction products. Lane 1, incubation using soluble proteins from *E. coli* harboring empty vector (pBAD/TOPO ThioFusion) and zeaxanthin (Zea); lanes 2 to 4, incubations using purified recombinant CsZCD and zeaxanthin, *cis*-violaxanthin (*cis*-Viol), and *trans*-violaxanthin (*trans*-Viol). Plates were sprayed with acidic dinitrophenylhydrazine to reveal the presence of carbonyl groups. The position of the reaction product is indicated by the arrowhead. As a result of the acidic conditions, 5,6-epoxy-carotenoids were converted to 5,8-epoxy-carotenoids, which appear as green to blue spots. OR refers to the origin.

(C) to **(E)** HPLC results and online diode-array spectra of CsZCD reaction products. The separation (monitored at 440 nm **[C]**) of zeaxanthin (peak 1) and its cleavage derivative (peak 3) and online diode-array spectra of peak 3 **(D)** and zeaxanthin **(E)** are shown. mAU, milliabsorbance units.

(F) to **(H)** UV-visible light spectra of the reaction product (peak 3) in hexane **(F)** and in ethanol before **(G)** and after **(H)** reduction with sodium borohydride.
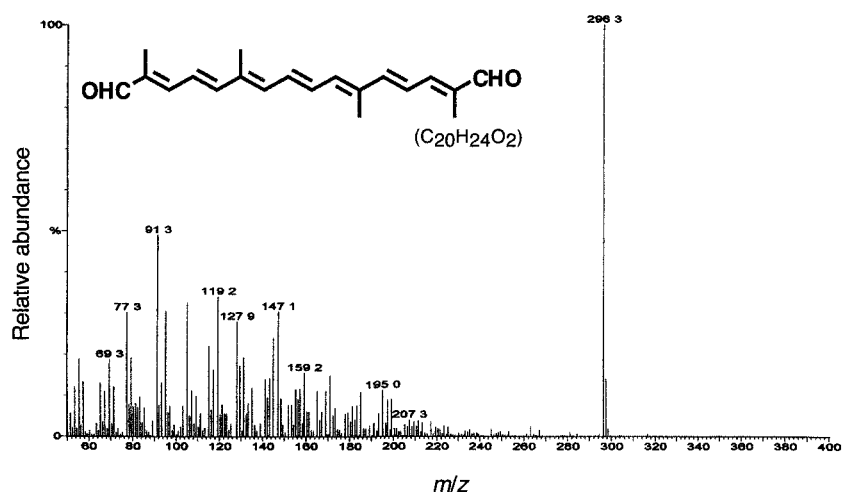
Figure 8. Full-Scan Mass Spectrometry of the Reaction Product of CsZCD.

Electron-impact mass spectrum of the reaction product (peak 3) obtained as shown in Figure 7C. m/z, mass-to-charge ratio.

compounds of saffron. On the other hand, CsZCD specifically catalyzed the cleavage of zeaxanthin at the 7,8 and 7′,8′ positions of the chromophore and thus initiated the formation of saffron secondary metabolites according to the sequential pathway shown in Figure 1C. Very similar enzyme activity has been described using a crude enzyme preparation from *Microcystis* (Jüttner and Höflatcher, 1985). It also has been observed that crocetin dialdehyde is a guanine apocarotenoid that accumulates in the flowers of *Jacquinia angustifolia* (Eugster et al., 1969) and in the roots of *Coleus forskohlii* (Tandon et al., 1979).

Although CsZCD is devoid of typical cleavable transit peptide (Gavel and von Heijne, 1990), our immunological data suggest that this enzyme is compartmentalized to the plastid. Precedence for this situation could be inferred from plastid enzymes remodeling membrane acyllipids, which are synthesized without transit peptides. These include the barley allene oxide synthase (Maucher et al., 2000) and the fatty acid hydroperoxide lyases of tomato (Froehlich et al., 2001) and alfalfa (Noordermer et al., 2000). In addition, these enzymes and *CsZCD* share the STVxR pattern in their N-terminal domains, whose role is not known at present.

The comparison between the enzymes mentioned above that remodel membrane acyllipids and *CsZCD* can be extended to their mode of action. Mechanistically, the homolytic hydroperoxide cleavage reaction catalyzed by allene oxide synthases and hydroperoxide lyases leads to the formation of an epoxide (Song et al., 1993) or is mediated by a transient epoxy carbocation (Noordermer et al., 2000). Similarly, for carotenoids, it has been observed that during vitamin A synthesis, the enzymatic cleavage of the central (15-15′) double bond of β-carotene is catalyzed by a monooxygenase en-

zyme via a transient carotene epoxide (Leuenberger et al., 2001).

Finally, comparison of the CsZCD amino acid sequence with the sequences of plant and mammalian carotenoid dioxygenases available in public databases revealed an overall similarity of 17 to 27%. This information can be used to define and narrow the catalytic domains of carotenoid dioxygenases and to identify their active residues.

Sequestration of Water-Soluble Carotenoid Metabolites

Carotenoids are lipophilic membrane components, and their accumulation in plants requires specialized chromoplast structures (Camara et al., 1995). Much less is known about carotenoid cleavage derivatives when they are synthesized in excess. In Crocus style branches, direct connections were observed between chromoplasts and the central vacuole (Figures 11D to 11F). Although convincing examples of interactions between plastids and vacuoles are rare, these have been observed in the gametophyte of the fern *Pteris vittata* and occasionally in a very limited group of higher plants, including the leaves of tomato (Crotty and Ledbetter, 1973) and *Hypoestes sanguinolenta* (Vaughn and Duke, 1981). Although the correlation of dynamic events and static electron micrographs is only tentative, it is suggested that in Crocus styles, carotenoid-derived metabolites become sequestered into vacuoles. In support of this possibility, cell suspension cultures of Crocus glycosylate exogenous crocetin and accumulate the resulting glycoside in vacuoles (Dufresne et al., 1999). This can be confirmed first by the polarity of crocetin glycosides found in the Crocus style
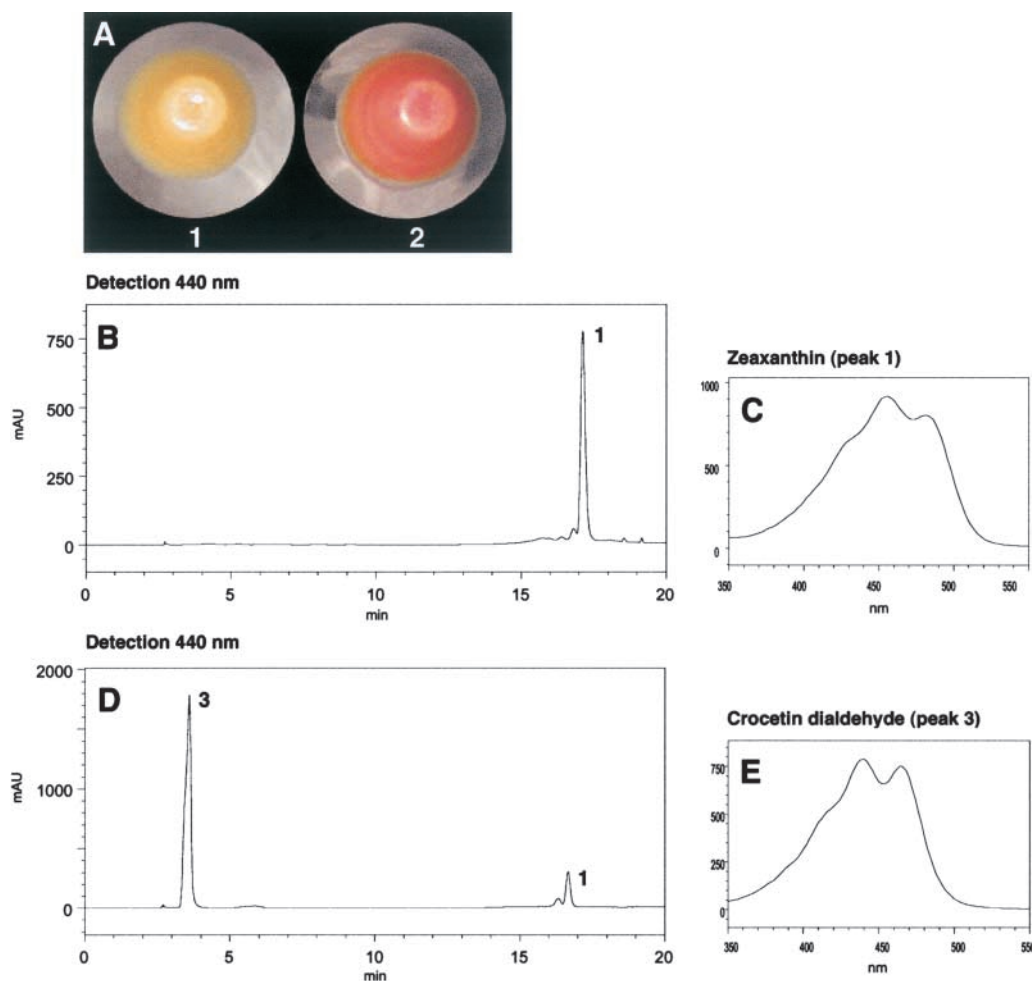
Figure 9. Plasmid-Based Assay of CsZCD in *E. coli*.

(A) Pellet of *E. coli* harboring the pCAR25delB plasmid, which allows zeaxanthin production alone (1) and after coexpression of CsZCD cDNA (2).
(B) to **(E)** HPLC results (monitored at 440 nm) and online diode-array spectra of the total lipid extract from *E. coli* harboring pCAR25delB plasmid
(**[B]** and **[C]**) and coexpressing CsZCD cDNA (**[D]** and **[E]**). mAU, milliabsorbance units.

tissue that conforms to the essential criterion of water solubility reported for vacuolar solutes (Frey-Wyssling, 1942; Matile, 1990; Jones and Vogt, 2001) and second by arbuscular mycorrhizal fungi that induce in root vacuoles the accumulation of mycorradicin (Klingner et al., 1995; Walter et al., 2000), which is a 10,10′-diapocarotene derived from the C_{14} dialdehyde produced by AtCCD1 (Schwartz et al., 2001) and CsCCD (this work). Sequestration of plastid-derived metabolites also has been observed in *Stevia rebaudiana*, which accumulates stevioside, a diterpenoid sweetner (Hanson and De Oliveira, 1993). The initial steps of stevioside biosynthesis occur in plastids and involve the cyclization of geranylgeranyl diphosphate into kaurene (Richman et al., 1999), which subsequently is oxidized, glycosylated, and seques-

tered in the vacuole as a water-soluble constituent (Kim et al., 1996). Finally, the sequestration of plastid-derived metabolites in vacuoles has been documented for chlorophyll catabolites (Hinder et al., 1996) through an ATP-binding cassette transporter (Lu et al., 1998).

Remodeling Carotenoids for New Functions

In plants, the biological roles of carotenoid-derived metabolites, except for abscisic acid, are not very well known. It has been shown that 3-hydroxy-β-ionone isolated from dwarf bean shoot inhibits the growth of lettuce seedlings (Kato-Noguchi et al., 1993). The sporulation and growth of the

pathogenic fungus *Peronospora tabacina* are inhibited by β-ionone (Schiltz, 1974), which protects tobacco plants from being infected by the same pathogen (Salt et al., 1986). Similarly, blumenin, a glycosylated cyclohexone produced from root carotenoids, inhibits fungal colonization and arbuscule formation during the initial stages of mycorrhiza development in barley and wheat (Fester et al., 1999). Finally, carotenoid-derived metabolites such as α-inone, β-ionone, and their related derivatives are important components of floral scents (Azuma et al., 2002) and could favor insect pollinization or constitute insect lures (Donaldson et al., 1990; Flath et al., 1994; McQuate and Peck, 2001). In addition to their potential biological functions in plants, carotenoid-derived

metabolites form important components of the aroma produced during flower and fruit development (Sefton et al., 1989; Eugster and Märki-Fischer, 1991; Winterhalter and Rouseff, 2002), during tea fermentation (Sanderson et al., 1971; Sefton et al., 1989), and during tobacco curing (Enzell,
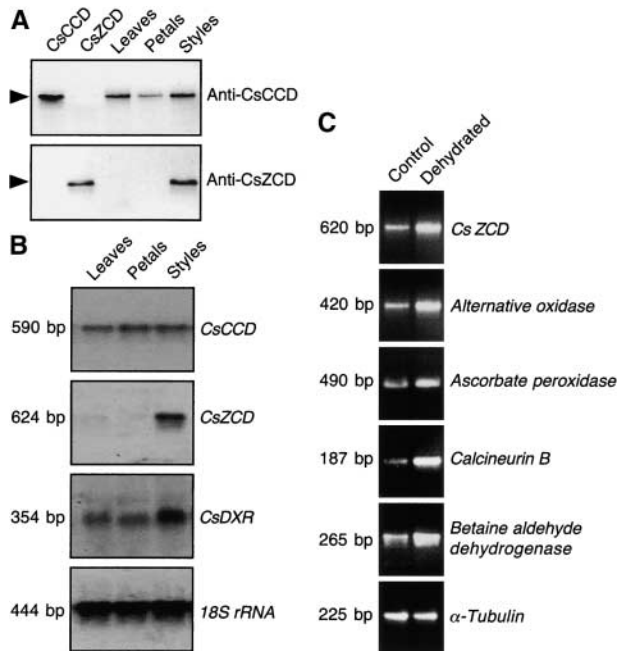
Figure 10. Molecular Analysis of CsCCD and CsZCD in Different Tissues of Crocus and during Dehydration Stress.

(A) Protein gel blot analysis of anti-CsCCD and anti-CsZCD antibody specificity and tissue-specific expression of CsCCD and CsZCD.
(B) RNA gel blot analysis and tissue-specific expression of *CsCCD*, *CsZCD*, and 1-deoxy-D-xylulose 5-phosphate reductoisomerase (*CsDXR*). A Crocus rRNA probe was used to check loading and transfer efficiency.
(C) RNA gel blot analysis of CsZCD and stress-regulated gene expression during dehydration. Crocus style branches were isolated from the perianth tubes and dehydrated on filter paper until half of their weight was lost. Total RNA then was used for reverse transcriptase–mediated PCR experiments. Shown are the ethidium bromide–stained gels from quantitative reverse transcriptase–mediated PCR experiments. The α-tubulin gene was used as a loading control.
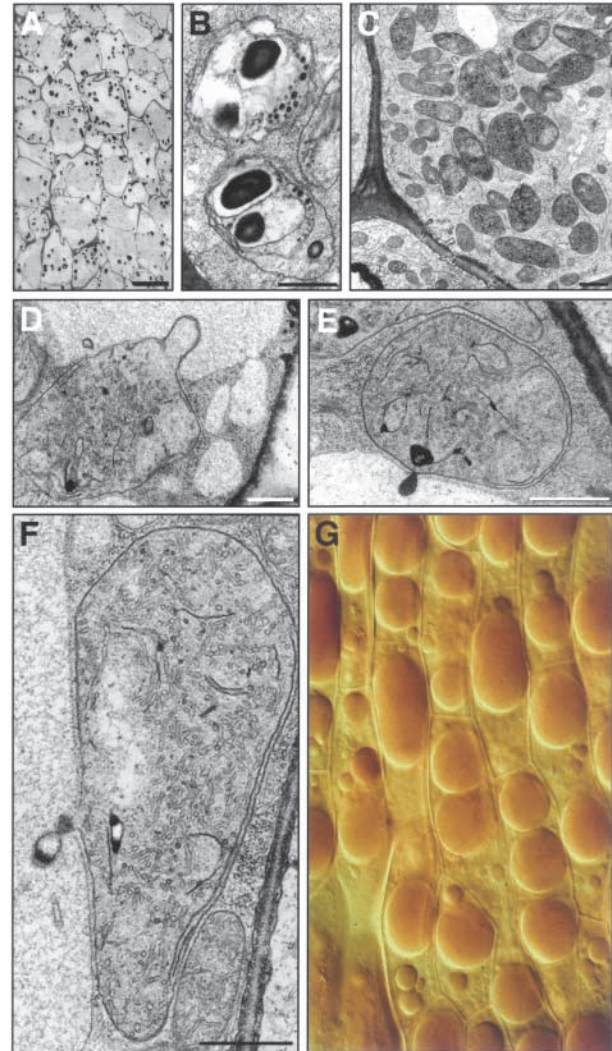

Figure 11. Amyloplast and Chromoplast Differentiation and Interactions between Chromoplasts and the Vacuole during the Biogenesis of Carotenoid-Derived Metabolites in Crocus Style Branches.

(A) Electron micrograph of style tissue showing electron-dense deposits after positive staining of polysaccharides. Bar = 10 μm.
(B) Details of amyloplasts showing that the electron-dense deposits are attributable to starch. Bar = 1 μm.
(C) Fully differentiated reticulotubular chromoplasts. Bar = 1 μm.
(D) to **(F)** Interaction between chromoplasts and vacuoles. Bars = 1 μm.
(G) Differential interference contrast microscopy observation of cells showing the central vacuole.

1985). Thus, the identification of specific enzymes that catalyze their formation could lead to a better appreciation of their biological role and to new biotechnological applications.

METHODS

Plant Material and Dehydration Treatments

Fresh flowers of *Crocus sativus* grown under field conditions in Porchères, France, were used throughout the experiment. To study the expression of genes induced by dehydration stress, the perianth tubes containing the floral tissues were removed from the corm and dehydrated on dry Whatman 3MM filter paper until half of their weight was lost. Control tissues were kept on hydrated Whatman 3MM filter paper for the same duration.

Chemicals

9-*cis*-Violaxanthin was isolated from ripe orange peel (Molnar and Szabolcs, 1980). *Trans*-violaxanthin and zeaxanthin were prepared as described previously (Camara, 1980; Bouvier et al., 1996).

cDNA Cloning of Carotenoid Cleavage Dioxygenase

Total RNA was isolated (Bouvier et al., 1998a) from Crocus style branches and poly(A$^+$) mRNAs were purified using Oligotex (Qiagen, Valencia, CA) before construction of a cDNA library in the λ Uni-ZAP XR vector (Stratagene) according to the manufacturer's instructions. Degenerated forward (5′-GC/T/C/GCAT/CCCA/T/CAAG/AG/CT/CG/C/TGAT/CCC-3′) and reverse (5′-TCA/GGTG/AATA/G/T/GCG/AAAG/ATCAT-3′) primers, corresponding to the AHPKVDP and HD-FAITE regions of the maize carotenoid dioxygenase Vp14 (Schwartz et al., 1997) and related putative carotenoid dioxygenases from pepper and *Synechocystis* sp PC6803, were used to prepare a screening probe by reverse transcriptase–mediated PCR (Bouvier et al., 1998b). Two amplified fragments, *CsCCD* (171 bp) and *CsZCD* (177 bp), were sequenced and showed a certain homology with carotenoid cleavage dioxygenases. Subsequently, ^{32}P-labeled *CsCCD* and *CsZCD* probes were used for plaque hybridization screening of the Crocus library according to standard procedures (Sambrook et al., 1989). Sequence analysis revealed that the longest clones corresponding to *CsCCD* (750 bp) and *CsZCD* (1200 bp) lacked the 5′ and 3′ regions that were obtained by rapid amplification of cDNA ends using the Gibco BRL kit, as described previously (Bouvier et al., 1998b).

Sequencing was performed using ABI 373 and ABI 3100 DNA sequencers (Applied Biosystems, Courtaboeuf, Paris, France). Sequence comparisons were performed through the National Center for Biotechnology Information using Basic Local Alignment Search Tool (BLAST) programs (Altschul et al., 1997).

Preparation of Anti-CsCCD and Anti-CsZCD Antibodies and Protein Gel Blot Analysis

Antibodies were developed in rabbits against synthetic peptides encompassing amino acids 121 to 133 (SRYVKKTSRLKQEE) of CsCCD and amino acids 216 to 229 (MARIDLRSGSVSRT) of CsZCD, to which C-terminal Cys residues were added. The synthetic peptides were conjugated to the maleimide-activated carrier protein keyhole limpet hemocyanin, as described previously (Nivison and Hanson, 1987).

Total protein was extracted from Crocus tissues (Van Etten et al., 1979) and quantified (Smith et al., 1985), and aliquots (50 μg) were used for SDS-PAGE. Proteins in the gel were transferred onto nitrocellulose membranes, which were probed with anti-CsCCD and anti-CsZCD antibodies at a concentration of 1:2500 in Tris-buffered saline plus Tween 20 and processed as described previously (Suire et al., 2000).

Analysis of Carotenoid-Derived Metabolites from Crocus Style Branches

The ethanol extract (50%) of freshly cut Crocus style branches (40 g) was used for pigment analysis. An aliquot of this extract was used for reverse-phase analysis using a Zorbax ODS column (4.6 mm × 25 cm; Interchim, France) and a SpectraSYSTEM (ThermoFinnigan, Les Ulis, France) comprising a SCM1000 solvent degasser, a P1-1000XR gradient pump, an AS3000 autosampler, and a UV6000LP diode-array detector. Data acquisition and processing were performed using ChromQuest version 3 software (ThermoFinnigan). The carotenoid-derived metabolites were eluted using two gradients. Gradient I (for the separation of zeaxanthin cleavage products) was as follows: 0 to 10 min, 25% acetonitrile in water to 100% acetonitrile at a flow rate of 1 mL/min. Gradient II (for the separation of zeaxanthin cleavage products and intact C_{40} carotenoids) was as follows: 0 to 20 min, 25% acetonitrile in water to 100% acetonitrile; 20 to 25 min, a linear gradient of acetonitrile to 100% dichloromethane; and 25 to 40 min, dichloromethane, at a flow rate of 1 mL/min. The different carotenoid derivatives were identified on the basis of HPLC retention times and UV-visible light spectra (Tarantilis et al., 1995; Pfister et al., 1996).

Production and Assay of Recombinant Carotenoid Cleavage Dioxygenases

Full-length CsCCD and CsZCD cDNAs were amplified by PCR using the forward and reverse primers 5′-ATGGGAGAAGTAGCGAAG-GAGG-3′ and 5′-TACGTCGGTTTGCTGCCACTGGAG-3′ for CsCCD and the forward and reverse primers 5′-ATGCAGGTGGACCCA-ACCAAGG-3′ and 5′-CTGCTGTGACAGCAGCTCAGCTTC-3′ for CsZCD. The resulting fragments were subcloned into pBAD/TOPO ThioFusion (Invitrogen, Carlsbad, CA), which allows translation of the polypeptide in a fusion with a 16-kD His-Patch thioredoxin under the control of an arabinose-inducible promoter. Transformed *Escherichia coli* (TOP10) was grown to an OD_{600} of 0.5 at 20 or 37°C in a Luria-Bertani medium containing ampicillin (100 μg/mL) before being induced with 0.02% arabinose and overnight culture. Bacterial cells were pelleted by centrifugation at 4°C and resuspended in 50 mM Tris-HCl, pH 7.5, containing 5 mM DTT before lysis by sonication (Bouvier et al., 1998b). The lysate was centrifuged at 10,000*g* to collect the supernatant containing the fusion protein. The expressed protein tended to form insoluble inclusion bodies when the induction temperature was maintained at 37°C. To overcome this problem, the temperature was decreased to 20°C. Soluble recombinant protein produced under these conditions was used for affinity chromatography at 4°C using ProBond resin (Invitrogen) as described by the manufacturer's protocol.

The purified protein (5 μg) or soluble protein (25 μg) from *E. coli* cells carrying the empty vector was incubated in a 200-μL assay mixture containing 5 μM FeSO$_4$, 25 to 100 μM carotenoid substrate, 0.2% octyl-β-glucoside, and 1 mM DTT buffered with 50 mM Tris-HCl, pH 7.6. After incubation at 30°C for 1 h, the reaction was stopped by adding 200 μL of acetone followed by 300 μL of dichloromethane:methanol (1:1 [v/v]). The mixture was centrifuged, and the hypophase was concentrated to dryness under a stream of nitrogen before thin layer chromatography. Silica gel plates were prepared with hexane:acetone (60:40 [v/v]), and the position of the reaction products was observed under UV-visible light before and after spraying the plate with a solution of acidic 2,4-dinitrophenylhydrazine to detect aldehydes and ketones (Stahl and Jork, 1965). HPLC separation of CsCCD reaction products was performed on a Zorbax ODS column (4.6 mm × 25 cm) as described above. A solvent gradient was used for elution as follows: 0 to 5 min, 80% acetonitrile in water; 5 to 10 min, 100% acetonitrile; 10 to 15 min, acetonitrile to 100% dichloromethane; and 15 to 20 min dichloromethane, at a constant flow rate of 1 mL/min. UV-visible light spectra were recorded at 374 and 440 nm. For CsZCD, the same column was used, and elution was accomplished with the following gradient: 0 to 10 min, acetonitrile; and 10 to 20 min, acetonitrile to 100% dichloromethane. The carotenoid cleavage products were identified by UV-visible spectrophotometry and mass spectrometry. Direct insertion probe mass spectrometry analysis was performed with a Trio 2000 mass spectrometer (Micromass, Manchester, UK). The ionizing voltage was 70 eV, and the temperature of the ion source chamber was 200°C.

E. coli Color Complementation

CsCCD and *CsZCD* cDNAs were amplified by PCR. The forward primer 5′-ATGGGAGAAGTAGCGAAGGAGG-3′ and the reverse primer 5′-TACGTCGGTTTGCTGCCACTGGAG-3′ were used for CsCCD, and the forward primer 5′-ATGCAGGTGGACCCAACC-AAGG-3′ and the reverse primer 5′-CTGCTGTGACAGCAGCTC-AGCTTC-3′ were used for CsZCD. The resulting fragments were ligated into the cloning site of the pBAD TOPO TA vector (Invitrogen), and the resulting plasmid was introduced into *E. coli* (strain JM109) carrying the zeaxanthin biosynthetic plasmid pCAR25delB (Misawa et al., 1990). Positive colonies were selected from the Luria-Bertani medium containing ampicillin (100 μg/mL) and chloramphenicol (50 μg/mL) and grown in liquid or solid Luria-Bertani medium before being induced with 0.02% arabinose. Carotenoid-derived metabolites from pelleted or scraped bacteria were extracted and analyzed as described for the in vitro assay.

Microscopy

For electron microscopy, the style tissues were fixed in 2.5% glutaraldehyde and postfixed in 1% OsO$_4$ in 0.1 M phosphate buffer at pH 7.2. The tissues were dehydrated in ethanol and stained with lead citrate and uranyl acetate after sectioning in Spurr resin. Photographs were taken with a Philips EM 300 electron microscope (Bordeaux, France). Polysaccharide visualization was performed according to a previously published procedure (Thiéry, 1967).

For immunohistochemistry, the tissue samples were fixed in 4% paraformaldehyde and 0.25% glutaraldehyde in PBS. The fixed tissues then were dehydrated in graded series of ethanol (50 to 99%) and subsequently infiltrated and embedded in paraffin. Sections of 10 μm were prepared and placed on microscope slides pretreated with 3-aminopropyltriethyoxysilane. Finally, the tissue sections were deparaffinized in xylene and rehydrated with decreasing concentrations of ethanol (99 to 50%) followed by water, PBS, and PBS containing 0.05% Triton X-100 and 1% BSA for 1 h before blocking with 5% goat serum to limit nonspecific binding. Blocked sections were incubated at 4°C overnight with primary CsCCD or CsZCD antibodies diluted 1:25 in PBS containing 0.01% Triton X-100 and 1% BSA. Control tissues were incubated with the appropriate preimmune serum under the same conditions. After washing with the same buffer, the sections were incubated for 1 h with diluted (1:200) Alexa-Fluor 488 goat anti-rabbit IgG conjugate (Molecular Probes Europe, Leiden, The Netherlands). After washing the sections with PBS, the samples were mounted in a medium containing PBS:glycerol (1v/1v) containing 1% ascorbic acid to reduce photobleaching. Labeled tissue sections were examined using a Zeiss LSM510 confocal laser-scanning microscope equipped with an Axiovert 100 inverted microscope (Jena, Germany). Excitation and emission wavelengths were 488 nm and 505 to 530 nm, respectively. The images were processed using Adobe Photoshop 5 (Adobe Systems, San Jose, CA).

Gene Expression Analysis

Total RNA was isolated from various Crocus organs and tissues using the NucleoSpin RNA Plant kit (Macherey-Nagel, Duren, Germany). RNA gel blot analysis was performed using ^{32}P-labeled Crocus probes as described previously (Bouvier et al., 1998a) using 25 μg of total RNA and a Crocus ribosomal 18S rRNA probe as internal controls for RNA loading. The gene expression induced by dehydration was analyzed three times by reverse transcriptase–mediated PCR. Total RNA (5 μg) was isolated and used for single-strand cDNA synthesis using Superscript II RNase H$^-$ reverse transcriptase (Gibco BRL) according to the manufacturer's protocol. An aliquot of the reaction mixture was used as a DNA template for PCR. The forward and reverse primers corresponding to the different Crocus genes used were as follows: *CsCCD*, 5′-ATGGATCTTCCTTTGTATTTCC-3′ and 5′-TTCGGATTTTATACCACGTTCACG-3′; *CsZCD*, 5′-GCCGTC-TTCCCCGACATCCAGATC-3′ and 5′-GCCTCCGCTCTTCTTCGA-TGATCG-3′; alternative oxidase, 5′-TTGGAGGAAGCGGAGAACGAG-CGG-3′ and 5′-GTGATATCCAACTGGAGCTGGATG-3′; ascorbate peroxidase, 5′-GTACCTCAAGGCGGTGGAGAAGTG-3′ and 5′-CCC-TGACCGATCCTTGTGACACC-3′; betaine aldehyde dehydrogenase, 5′-GATACGCGTTATGGCTTAGGTGG-3′ and 5′-AAGCTT-GGAAGGTGGGGTATACC-3′; calcineurin B, 5′-ATGGGGTGCTTT-CAGTCCAAGTCG-3′ and 5′-AAATAAAGCAAGCTGAAATTCTTCC-3′; and 1-deoxy-D-xylulose 5-phosphate reductoisomerase, 5′-GGA-TGTGCCGGTTTAAAGCCTACTG-3′ and 5′-AGACCCTTTATTGAA-AAGGGTAGC-3′. Crocus α-tubulin probe amplified using the forward and reverse primers 5′-ATGATTTCCAACTCGACCAGTGTC-3′ and 5′-ATACTCATCACCCTCGTCACCATC-3′ was used as an endogenous control. PCR products were separated by electrophoresis on 1.5% agarose gels before detection using ethidium bromide.

Upon request, all new materials described in this article will be made available in a timely manner for noncommercial research purposes.

Accession Numbers

The GenBank accession numbers for the cDNAs mentioned in this article are as follows: CsCCD, AJ132927; CsZCD, AJ489276;

alternative oxidase, AJ489270; ascorbate peroxidase, AJ489279; betaine aldehyde dehydrogenase, AJ489271; calcineurin B, AJ489272; α-tubulin, AJ489275; 1-deoxy-D-xylulose 5-phosphate reductoisomerase, AJ489274; ribosomal 18S rRNA, AJ489273; Vp14, U95953; pepper CaCCD, Y14164; *Synechocystis* sp PC6803, 90917, Sll1541, Sll0572, and Slr1648; partial EST from Crocus, CAC95132; partial Crocus EST, CAC95133; and Md-FS2, CAB07784.

REFERENCES

Altschul, S.F., Madden, T.L., Schäffer, A.A., Zhang, J., Zhang, Z., Miller, W., and Lipman, D.J. (1997). Gapped BLAST and PSI-BLAST: A new generation of protein database search programs. Nucleic Acids Res. **25,** 3389–3402.

Azuma, H., Toyota, M., Asakawa, Y., Takaso, T., and Tobe, H. (2002). Floral scent chemistry of mangrove plants. J. Plant Res. **115,** 47–53.

Bosser, A., and Belin, J.M. (1994). Synthesis of β-ionone in an aldehyde/xanthine oxidase/β-carotene system involving free radical formation. Biotechnol. Prog. **10,** 129–133.

Bouvier, F., Backhaus, R.A., and Camara, B. (1998a). Induction and control of chromoplast-specific carotenoid genes by oxidative stress. J. Biol. Chem. **273,** 30651–30659.

Bouvier, F., d'Harlingue, A., Hugueney, P., Marin, E., Marion-Poll, A., and Camara, B. (1996). Xanthophyll biosynthesis: Cloning, expression, functional reconstitution, and regulation of β-cyclohexenyl carotenoid epoxidase from pepper (*Capsicum annuum*). J. Biol. Chem. **271,** 28861–28867.

Bouvier, F., d'Harlingue, A., Suire, C., Backhaus, R.A., and Camara, B. (1998b). Dedicated roles of plastid transketolases during the early onset of isoprenoid biogenesis in pepper fruits. Plant Physiol. **117,** 1423–1431.

Buchecker, R., and Eugster, C.H. (1973). Absolute Konfiguration von Picrocrocin. Helv. Chim. Acta **56,** 1121–1124.

Buttery, R.G., Teranishi, R., Ling, L.C., Flath, R.A., and Stern, D.J. (1988). Quantitative studies on origins of fresh tomato aroma volatiles. J. Agric. Food Chem. **36,** 1247–1250.

Camara, B. (1980). Biosynthesis of keto-carotenoids in *Capsicum annuum* fruits. FEBS Lett. **118,** 315–318.

Camara, B., Hugueney, P., Bouvier, F., Kuntz, M., and Monéger, R. (1995). Biochemistry and molecular biology of chromoplast development. Int. Rev. Cytol. **163,** 175–247.

Critchley, J.P., Friend, J., and Swain, T. (1958). A micro-method for differentiating between conjugated aldehydes and ketones. Chem. Ind. 596–597.

Crotty, W.J., and Ledbetter, M.C. (1973). Membrane continuities involving chloroplast and other organelles in plant cells. Science **182,** 839–841.

Donaldson, J.M.I., McGovern, T.P., and Ladd, T.L.J. (1990). Floral attractants for the Cetoniinae and Rutelinae (Coleoptera: Scarabaeidae). J. Econ. Entomol. **83,** 1298–1305.

Dufresne, C., Cormier, F., Dorion, S., Higgli, U.A., Pfister, S., and Pfander, H. (1999). Glycosylation of encapsulated crocetin by a *Crocus sativus* L. cell culture. Enzyme Microb. Technol. **24,** 453–462.

El-Tinay, A.H., and Chichester, C.O. (1970). Oxidation of β-carotene: Site of initial attack. J. Org. Chem. **35,** 2290–2293.

Enzell, C. (1985). Biodegradation of carotenoids: An important route to aroma compounds. Pure Appl. Chem. **57,** 693–700.

Enzell, C.R., Francis, G.W., and Laaen-Jensen, S. (1969). Mass spectrometric studies of carotenoids. 2. A survey of fragmentation reactions. Acta Chem. Scand. **23,** 727–750.

Eugster, C.H., Hürlimann, H., and Leuenberger, H.J. (1969). Crocetindialdehyd und Crocetinhalbaldehyd als Blütenfarbstoffe von *Jacquinia angustifolia*. Helv. Chim. Acta **52,** 89–90.

Eugster, C.H., and Märki-Fischer, E. (1991). The chemistry of rose pigments. Angew. Chem. Int. Ed. Engl. **30,** 654–672.

Fester, T., Maier, W., and Strack, D. (1999). Accumulation of secondary compounds in barley and wheat roots in response to inoculation with arbuscular mycorrhizal fungus and co-inoculation with rhizosphere bacteria. Mycorrhiza **8,** 241–246.

Flath, R.A., Cunningham, R.T., Liquido, N.J., and McGovern, T.P. (1994). Alpha-ionol as attractant for trapping *Batrocera latifrons* (Diptera: Tephritidae). J. Econ. Entomol. **87,** 1470–1476.

Fleischmann, P., Studer, K., and Winterhalter, P. (2002). Partial purification and kinetic characterization of a carotenoid cleavage enzyme from quince fruit (*Cydonia oblonga*). J. Agric. Food Chem. **50,** 1677–1680.

Frey-Wyssling, A. (1942). Zur Physiologie der pflanzlichen Glukoside. Naturwissenschaften **30,** 500–503.

Froehlich, J.E., Itoh, A., and Howe, G.A. (2001). Tomato allene oxide synthase and fatty acid hydroperoxide lyase, two cytochrome P450s involved in oxylipin metabolism, are targeted to different membranes of chloroplast envelope. Plant Physiol. **125,** 306–317.

Gainer, J.L., and Brumgard, F.B. (1982). Using excess volume of mixing to correlate diffusivities in liquids. Chem. Eng. Commun. **15,** 323–329.

Gavel, Y., and von Heijne, G. (1990). A conserved cleavage-site motif in chloroplast transit peptides. FEBS Lett. **261,** 455–458.

Gross, J., and Eckhardt, G. (1981). Structures of persicaxanthin, persicachrome and other apocarotenoids of various fruits. Phytochemistry **20,** 2267–2269.

Hanson, J.R., and De Oliveira, B.H. (1993). Stevioside and related sweet diterpenoid glycosides. Nat. Prod. Rep. **10,** 301–309.

Hinder, B., Schellenberg, M., Rodoni, S., Ginsburg, S., Vogt, E., Martinoia, E., Matile, P., and Hörtensteiner, S. (1996). How plants dispose of chlorophyll catabolites. J. Biol. Chem. **271,** 27233–27236.

Holloway, G.M., and Gainer, J.L. (1988). The carotenoid crocetin enhances pulmonary oxygenation. J. Appl. Physiol. **65,** 683–686.

Ishitani, M., Nakamura, T., Han, S.Y., and Takabe, T. (1995).

Expression of the betaine aldehyde dehydrogenase gene in barley in response to osmotic stress and abscisic acid. Plant Mol. Biol. **27,** 307–315.

Isler, O., Gutmann, H., Lindlar, H., Montavon, M., Rüegg, R., Ryser, G., and Zeller, P. (1956). Synthesen in der Carotinoid-Reihe. 6. Synthese von crocetindialdhyd und lycopin. Helv. Chim. Acta **39,** 463–473.

Jones, P., and Vogt, T. (2001). Glycosyltransferases in secondary plant metabolism: Tranquilizers and stimulant controllers. Planta **213,** 164–174.

Jüttner, F., and Höflatcher, B. (1985). Evidence of β-carotene 7,8(7′,8′) oxygenase (β-cyclocitral, crocetindial generating) in *Microcystis*. Arch. Microbiol. **141,** 337–343.

Kato-Noguchi, H., Kosemura, S., Yamamura, S., and Hasegawa, K. (1993). A growth inhibitor, R-(−)-3-hydroxy-β-ionone, from light-grown shoots of a dwarf cultivar of *Phaseolus vulgaris*. Phytochemistry **33,** 553–555.

Kawakami, M., and Kobayashi, A. (2002). Carotenoid-derived aroma compounds in tea. In Carotenoid-Derived Aroma Compounds, P. Winterhalter and R.L. Rouseff, eds (Washington, DC: American Chemical Society), pp. 145–159.

Kim, K.K., Sawa, Y., and Shibata, H. (1996). Hydroxylation of *ent*-kaurenoic acid to steviol in *Stevia rebaudiana* Bertoni: Purification and partial characterization of the enzyme. Arch. Biochem. Biophys. **332,** 223–230.

Klingner, A., Bothe, H., Wray, V., and Marner, F.J. (1995). Identification of a yellow pigment formed in maize roots upon mycorrhizal colonization. Phytochemistry **38,** 53–55.

Kudla, J., Xu, Q., Harter, K., Gruissem, W., and Luan, S. (1999). Genes for calcineurin B-like proteins in *Arabidopsis* are differentially regulated by stress signals. Proc. Natl. Acad. Sci. USA **96,** 4718–4723.

Leuenberger, M.G., Engeloch-Jarret, C., and Woggon, W.D. (2001). The reaction mechanism of the enzyme-catalyzed central cleavage of β-carotene to retinal. Angew. Chem. Int. Ed. **40,** 2614–2617.

Liao, Y.H., Houghton, P.J., and Hoult, J.R.S. (1999). Novel and known constituents from *Buddleja* species and their activity against leukocyte eicosanoid generation. J. Nat. Prod. **62,** 1241–1245.

Lu, Y.P., Li, Z.S., Drozdowicz, Y.M., Hörtensteiner, S., Martinoia, E., and Rea, P.A. (1998). AtMRP2, an *Arabidopsis* ATP binding cassette transporter able to transport glutathione S-conjugates and chlorophyll catabolites: Functional comparisons with Atmrp1. Plant Cell **10,** 267–282.

Lutz, A., and Winterhalter, P. (1992). Bio-oxidative cleavage of carotenoids: Important route to physiological active plant constituents. Tetrahedron Lett. **33,** 5169–5172.

Maoka, T., Fujiwara, Y., Hashimoto, K., and Akimoto, N. (2001). Isolation of a series of apocarotenoids from the fruits of the red paprika *Capsicum annuum* L. J. Agric. Food Chem. **49,** 1601–1606.

Märki-Fischer, E., and Eugster, C.H. (1988). Rosafluin, ein neues Diapocarotindiol aus Rosenblüten. Helv. Chim. Acta **71,** 1491–1497.

Mathew, B. (1983). The Crocus. (Portland, OR: Timber Press).

Matile, P. (1990). The toxic compartment of plant cell. In Progress in Plant Cellular and Molecular Biology, H.J.J. Nijkamp, L.H.W. Van Der Plas, and U.U.V. Van Aartrijk, eds (Dordrecht, The Netherlands: Kluwer Academic Publishers), pp. 557–566.

Maucher, H., Hause, B., Feussner, I., Ziegler, J., and Wasternack, C. (2000). Allene oxide synthases of barley (*Hordeum vulgare* cv. Salome): Tissue specific regulation in seedling development. Plant J. **21,** 199–213.

Maxwell, D.P., Wang, Y., and McIntosh, L. (1999). The alternative oxidase lowers mitochondrial reactive oxygen production in plant cells. Proc. Natl. Acad. Sci. USA **96,** 8271–8276.

McQuate, G.T., and Peck, S.L. (2001). Enhancement of attraction of alpha-ionol to male *Bactrocera latifrons* (Diptera: Tephritidae) by addition of a synergist, cade oil. J. Econ. Entomol. **94,** 39–46.

Misawa, N., Nakagawa, M., Kobayashi, K., Yamano, S., Izawa, K., Nakamura, K., and Harashima, K. (1990). Elucidation of the *Erwinia uredovora* carotenoid biosynthetic pathway by functional analysis of gene products expressed in *Escherichia coli*. J. Bacteriol. **172,** 6704–6712.

Mittler, R., and Zilinskas, B.A. (1994). Regulation of pea cytosolic ascorbate peroxidase and other antioxidant enzymes during the progression of drought stress and following recovery from drought. Plant J. **5,** 397–405.

Molnar, P., and Szabolcs, J. (1980). β-Citraurin epoxide, a new carotenoid from Valencia orange peel. Phytochemistry **19,** 633–637.

Nivison, H.T., and Hanson, M.R. (1987). Production and purification of synthetic peptide antibodies. Plant Mol. Biol. Rep. **5,** 295–309.

Noordermer, M.A., van Dijken, A.J.H., Smeekens, S.C.M., Veldink, G.A., and Vliegenthart, J.F.G. (2000). Characterization of three cloned and expressed 13-hydroperoxide lyase isoenzymes from alfalfa with unusual N-terminal sequences and different enzyme kinetics. Eur. J. Biochem. **267,** 2473–2482.

Pfander, H., and Schurtenberger, H. (1982). Biosynthesis of C_{20}-carotenoids in *Crocus sativus*. Phytochemistry **21,** 1039–1042.

Pfister, S., Meyer, P., Steck, A., and Pfander, H. (1996). Isolation and structure elucidation of carotenoid-glycosyl esters in *Gardenia* fruits (*Gardenia jasminoides* Ellis) and saffron (*Crocus sativus* Linne). J. Agric. Food Chem. **44,** 2612–2615.

Richman, A.S., Gijzen, M., Starratt, A.N., Yang, Z., and Brandle, J.E. (1999). Diterpene synthesis in *Stevia rebaudiana*: Recruitment and up-regulation of key enzymes from the gibberellin biosynthetic pathway. Plant J. **19,** 411–421.

Salt, S.D., Tuzun, S., and Kuc, J. (1986). Effect of β-ionone and abscisic acid on the growth of tobacco and resistance to blue mold: Mimicry of effects of stem infection by *Peronospora tabacina* Adam. Physiol. Mol. Plant Pathol. **28,** 287–297.

Sambrook, J., Fritsch, E.F., and Maniatis, T. (1989). Molecular Cloning: A Laboratory Manual. (Cold Spring Harbor, NY: Cold Spring Harbor Laboratory Press).

Sampathu, S.R., Shivashankar, S., and Lewis, Y.S. (1984). Saffron (*Crocus sativus* Linne): Cultivation, processing, chemistry and standardization. Crit. Rev. Food Sci. Nutr. **20,** 123–157.

Sanderson, G.W., Co, H., and Gonzalez, J.G. (1971). Biochemistry of tea fermentation: The role of carotenes in black tea aroma formation. J. Agric. Food Chem. **36,** 231–236.

Schiltz, P. (1974). Action inhibitrice de la β-ionone au cours du développement de *Peronospora tabacina*. Ann. Tabac **11,** 207–216.

Schwartz, S.H., Qin, X., and Zeevaart, J.A.D. (2001). Characterization of a novel carotenoid cleavage dioxygenase. J. Biol. Chem. **276,** 25208–25211.

Schwartz, S.H., Tan, B.C., Gage, D.A., Zeevaart, J.A.D., and McCarty, D.R. (1997). Specific oxidative cleavage of carotenoids by VP14 of maize. Science **276,** 1872–1874.

Sefton, M.A., Skouroumounis, G.K., Massy-Westropp, R.A., and Williams, P.J. (1989). Norisoprenoids in *Vitis vinifera* white wine

grapes and the identification of a precursor of damascenone in these fruits. Aust. J. Chem. **42,** 2071–2084.

Smith, P.K., Krohn, R.I., Hermanson, G.T., Mallia, A.K., Gartner, F.H., Provenzano, M.D., Fujimoto, E.K., Goeke, N.M., Olson, B.J., and Klenk, D.C. (1985). Measurement of protein using bicinchoninic acid. Anal. Biochem. **150,** 76–85.

Song, W.C., Baertschi, S.W., Boeglin, W.E., Harris, T.M., and Brash, A.R. (1993). Formation of epoxyalcohols by a purified allene oxide synthase: Implications for the mechanism of allene oxide synthesis. J. Biol. Chem. **268,** 6293–6298.

Stahl, E., and Jork, H. (1965). Terpene derivatives, essentials oils, balsams, and resins. In Thin-Layer Chromatography: A Laboratory Handbook, E. Stahl, ed (Berlin: Springer-Verlag), pp. 186–210.

Straubinger, M., Bau, B., Eckstein, S., Fink, M., and Winterhalter, P. (1998). Identification of novel glycosidic aroma precursors in saffron (*Crocus sativus* L.). J. Agric. Food Chem. **46,** 3238–3242.

Suire, C., Bouvier, F., Backhaus, R.A., Bégu, D., Bonneu, M., and Camara, B. (2000). Cellular localization of isoprenoid biosynthetic enzymes in *Marchantia polymorpha*: Uncovering a new role of oil bodies. Plant Physiol. **124,** 971–978.

Tandon, J.S., Katti, S.B., Rüedi, P., and Eugster, C.H. (1979). Crocetin-dialdehyde from *Coleus forskolii* Briq., Labiatae. Helv. Chim. Acta **274,** 2706–2707.

Tarantilis, P.A., Tsoupras, G., and Polissiou, M.G. (1995). Determination of saffron (*Crocus sativus* L.) components in crude plant extract using high-performance liquid chromatography-UV-visible photodiode-array detection-mass spectrometry. J. Chromatogr. **699,** 107–118.

Thiéry, J.P. (1967). Mise en évidence des polysaccharides sur des coupes fines en microscopie électronique. J. Microsc. **6,** 987–1018.

Van Etten, J.L., Freer, S.N., and McCune, B.K. (1979). Presence of a major (storage?) protein in dormant spores of the fungus *Botryodiplodia theobromae*. J. Bacteriol. **138,** 650–652.

Vaughn, K.C., and Duke, S.O. (1981). Evaginations from the plastid envelope: A method for transfer of substances from plastid to vacuole. Cytobios **32,** 89–95.

Vetter, W., Englert, G., Rigassi, N., and Schwieter, U. (1971). Spectroscopic methods. In Carotenoids, O. Isler, ed (Basel, Switzerland: Birkhäuser Verlag), pp. 189–266.

von Lintig, J., and Vogt, K. (2000). Filling a gap in vitamin A research: Molecular identification of an enzyme cleaving β-carotene to retinal. J. Biol. Chem. **275,** 11915–11920.

Wahlberg, I., Karlsson, K., Austin, D.J., Junker, N., Roeraade, J., and Enzell, C.R. (1977). Effects of flue-curing and ageing on the volatile, neutral and acidic constituents of Virginia tobacco. Phytochemistry **16,** 1217–1231.

Walter, M.H., Fester, T., and Strack, D. (2000). Arbuscular mycorrhizal fungi induce the non-mevalonate methylerythritol phosphate pathway of isoprenoid biosynthesis correlated with accumulation of the "yellow pigment" and other apocarotenoids. Plant J. **21,** 571–578.

Watillon, B., Kettmann, R., Arredouani, A., Hecquet, J.F., Boxux, P., and Burny, A. (1998). Apple messenger RNAs related to bacterial lignostilbene dioxygenase and plant SAUR genes are preferentially expressed in flowers. Plant Mol. Biol. **36,** 909–915.

Winterhalter, P., and Rouseff, R.L. (2002). Carotenoid-Derived Aroma Compounds. (Washington, DC: American Chemical Society).

Winterhalter, P., and Straubinger, M. (2000). Saffron: Renewed interest in an ancient spice. Food Rev. Int. **16,** 39–59.

Wu, Z., Robinson, D.S., Hughes, R.K., Casey, R., Hardy, D., and West, S.I. (1999). Co-oxidation of β-carotene catalyzed by soybean and recombinant pea lipoxygenase. J. Agric. Food Chem. **47,** 4899–4906.

Wyss, A., Wirtz, G., Woggon, W.D., Brugger, R., Wyss, M., Friedlein, A., Bachmann, H., and Hunziker, W. (2000). Cloning and expression of β,β-carotene 15,15′-dioxygenase. Biochem. Biophys. Res. Commun. **271,** 334–336.

Oxidative Remodeling of Chromoplast Carotenoids: Identification of the Carotenoid Dioxygenase CsCCD and CsZCD Genes Involved in Crocus Secondary Metabolite Biogenesis

Florence Bouvier, Claude Suire, Jérôme Mutterer and Bilal Camara

This information is current as of July 9, 2017

References	This article cites 77 articles, 21 of which can be accessed free at: /content/15/1/47.full.html#ref-list-1
Permissions	https://www.copyright.com/ccc/openurl.do?sid=pd_hw1532298X&issn=1532298X&WT.mc_id=pd_hw1532298X
eTOCs	Sign up for eTOCs at: http://www.plantcell.org/cgi/alerts/ctmain
CiteTrack Alerts	Sign up for CiteTrack Alerts at: http://www.plantcell.org/cgi/alerts/ctmain
Subscription Information	Subscription Information for *The Plant Cell* and *Plant Physiology* is available at: http://www.aspb.org/publications/subscriptions.cfm